

# Aeroelastic Sensitivity Analysis of Wings Using Automatic Differentiation

Jason Cherian Issac\* and Rakesh K. Kapania†

*Virginia Polytechnic Institute and State University, Blacksburg, Virginia 24061-0203*

Flutter analysis of a general wing is carried out using finite element structural modeling (MSC/NASTRAN), a subsonic kernel function unsteady aerodynamics and a  $V$ - $g$  type of solution (FAST). The shape of the wing cross section is generated by parameterization using the Joukowski transformation, so that shapes of varying thickness and camber can be obtained by varying the parameters. The CQUAD4 (quadrilateral) and CTRIA3 (triangular) membrane-bending shell elements, the CBAR beam element and the CSHEAR shear panel element from MSC/NASTRAN have been used in this study. The validation of finite element modeling is done by performing dynamic analysis of an AGARD swept wing model. The sensitivity of flutter speed of the wing to shape parameters, namely, aspect ratio, area, taper ratio, and sweep angle is obtained using a central difference scheme in conjunction with automatic differentiation (ADIFOR). The sensitivity of flutter speed to modal parameters, namely, natural frequency, generalized mass, and generalized aerodynamic forces is computed using ADIFOR.

## Introduction

**S**ENSITIVITY analysis is an important tool, which yields information about the dependence of the aeroelastic instability on the design parameters of the wing. In today's design environment, affordability drives the design process. Sensitivity analysis and optimization techniques that make use of sensitivity information will be very useful to reduce the cost of the design and the cost of the design process. The structural and aerodynamic characteristics of a wing are functions of its shape and, hence, the flutter response is sensitive to changes in shape parameters. The sensitivity derivatives of the flutter speed with respect to modal parameters of the wing enable one to make a judicious choice of the number of modes that are required for flutter analysis for a reasonable estimate of the flutter speed.

Automatic differentiation is emerging as a valuable tool for sensitivity calculations. ADIFOR, GRESS, PADRE-2, power calculus, and ODYSEE are some of the automatic differentiation packages<sup>1</sup> developed for differentiating Fortran 77 codes. ADIFOR is a joint venture of Rice University and Argonne National Laboratory. ADIFOR processes a given Fortran code and generates a Fortran code for computing the derivatives of the desired output variables with respect to the independent variables by applying the chain rule of differentiation. Automatic differentiation can handle codes of arbitrary size and produce exact derivatives of the discrete system with no truncation error. This paper will help to introduce the benefits of ADIFOR to the design community.

Though equivalent plate representation in conjunction with global Ritz analysis techniques<sup>2-5</sup> are relatively inexpensive for mathematical modeling of wings to study aeroelasticity, finite element methods (FEM) are being used in industry for structural modeling of aircraft wings. Several commercial finite element codes like ABAQUS, ANSYS, EAL, IDEAS, and NASTRAN exist for finite element analysis of structures. The current work focusses on modeling the wing structure using MSC/NASTRAN.<sup>6</sup> One of the features of using FEM is that any planform shape and wing cross section could be analyzed, as opposed to the Rayleigh-Ritz formulation based equivalent plate model,<sup>3,4</sup> where only a trapezoidal skewed configuration of uniform thickness and layerwise construction could be analyzed. The wing skins, spars, and ribs of an airplane wing can be modeled using shell and beam elements in MSC/NASTRAN.

Received March 9, 1996; revision received Nov. 22, 1996; accepted for publication Nov. 25, 1996; also published in *AIAA Journal on Disc*, Volume 2, Number 2. This paper is declared a work of the U.S. Government and is not subject to copyright protection in the United States.

\*Postdoctoral Fellow, Aerospace and Ocean Engineering, Multidisciplinary Analysis and Design Center for Advanced Vehicles. Student Member AIAA.

†Professor, Aerospace and Ocean Engineering, Multidisciplinary Analysis and Design Center for Advanced Vehicles. Associate Fellow AIAA.

In this paper, validation of finite element modeling using MSC/NASTRAN is done for dynamic analysis of a swept wing, and the results are compared with previously published results. To encourage the use of the new methods presented, they are implemented using industry standard tools such as MSC/NASTRAN. The airfoil shape is generated by transforming a circle into an airfoil so that shapes of varying thickness and camber can be obtained by varying the parameters. Finite element discretization of the wing skins, spars, and ribs is done, and a free vibration analysis of the wing is performed. The natural frequencies and mode shapes obtained are used to generate the generalized aerodynamic forces required for flutter analysis using FAST,<sup>7</sup> which employs subsonic kernel function unsteady aerodynamics. The sensitivity of flutter speed to shape and modal parameters is computed using a combination of central difference scheme and automatic differentiation software ADIFOR. Optimization techniques that use these sensitivity derivatives are useful in the design stage, and these can be integrated into the design process for an optimum design.

## Dynamic Analysis of a Swept Wing

To validate the modeling, a swept back wing model reported in Ref. 8 is analyzed. It is an all aluminum wing, swept back by 30 deg and has five identical spars and three identical ribs bonded to the top and bottom cover skins. The dimensions of the wing and its cross-sectional properties are given in Fig. 1. The finite element discretization of the wing is given in Fig. 2.

The natural frequencies of the wing are calculated using MSC/NASTRAN. The wing skins are modeled using CQUAD4 and CTRIA3 shell membrane-bending elements, and the spar and rib caps are modeled using CBAR beam elements. However, the spar and rib webs are modeled in two different ways: 1) using CSHEAR shear panel elements and 2) using CQUAD4 shell membrane-bending elements. The natural frequencies of the wing are compared in Table 1 to the results reported in Ref. 5, which were computed using ELFINI finite element package. Note that in the finite element model reported in Ref. 5, the webs act only in shear. The results obtained using shear panels for the webs compare well with ELFINI results. When shear panels are used to model the webs, it is assumed that the webs act only in shear and the required axial stiffness at the edges are provided to support the corner forces. However, these webs also contribute to the stiffness of the structure in a small way. Hence, the spar and rib webs are modeled using CQUAD4 shell membrane-bending elements and the first five frequencies are given in Table 1. The CQUAD4 element for the webs gives stiffer solutions, as can be seen from Table 1 (the frequencies of transverse vibration are about 2–3% higher, especially in the bending modes, and the in-plane frequency is also higher).

When using the CSHEAR element in MSC/NASTRAN (Fig. 3), appropriate factors  $F_1$  and  $F_2$  have to be specified for providing extensional stiffness along the sides of the element to handle the corner forces, which are parallel to the sides of the element.  $F_1$  is the effectiveness factor for extensional stiffness along edges 1–2 and 3–4, and  $F_2$  is the effectiveness factor for extensional stiffness along edges 2–3 and 1–4. The effective extensional area is defined by means of extensional rods on the perimeter of the element. Thus,

if  $F_1 = 1.0$ , the panel is fully effective for extension in the 1–2 and 3–4 direction. The areas of the rods on the edges 1–2 and 3–4 are set equal to  $(0.5 F_1 T w_1)$ , where  $w_1$  is the average width of the panel and  $T$  is the thickness of the panel. Proper selection of the effectiveness factors is important when using the shear panel elements. Three different cases were examined using the effectiveness factors. If the default values of  $F_1 = F_2 = 0.0$  are used, then the computed frequencies are very small because the shear panel elements have no axial stiffness along the edges. If the panels are made fully effective for extension in both directions, then the solution obtained is much stiffer than that obtained using CQUAD4 shell membrane-bending

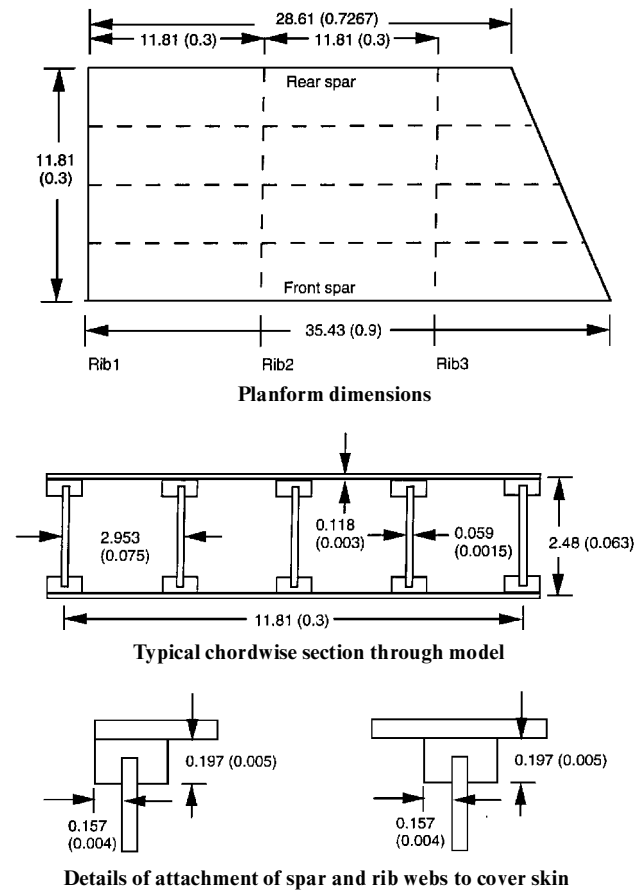


Fig. 1 Planform dimensions and cross-sectional properties of the wing. All dimensions are in inches (meters).

Table 1 Natural frequencies of the AGARD swept wing model

Mode number	Frequencies, Hz		
	Present (CSHEAR)	Livne <sup>5</sup>	Present (CQUAD4)
1 (1st bending)	116.8	115.6	120.8
2 (in plane)	318.0	317.6	353.0
3 (1st torsion)	415.4	418.4	416.9
4 (2nd bending)	579.5	576.4	593.1
5 (2nd torsion)	1082.3	1086.0	1094.3

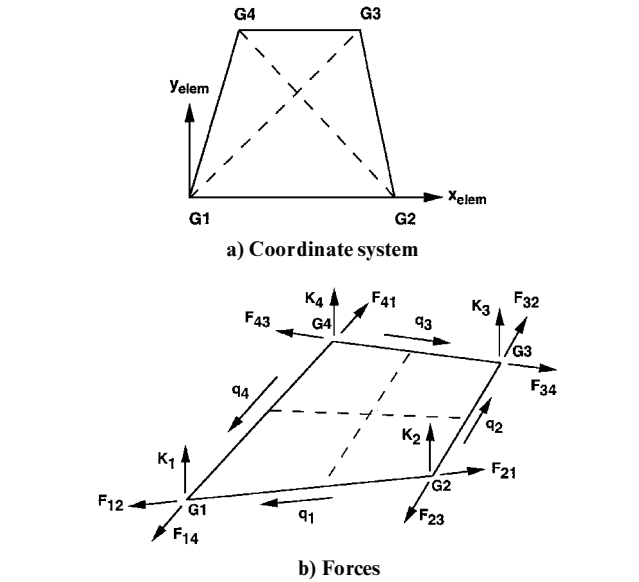


Fig. 3 CSHEAR element.

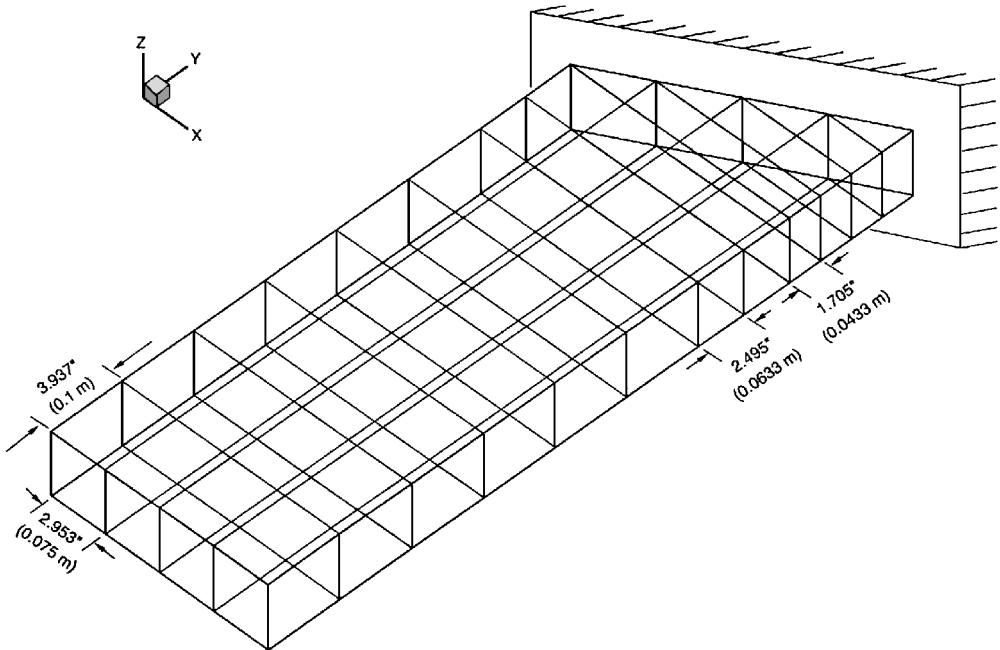


Fig. 2 Finite element discretization of the AGARD swept back wing model.

elements for the webs. The proper choice is to make the panel (for spar and rib webs) fully effective for extension in the transverse direction of the wing and let the spar and rib caps carry the load in the other direction. This gives frequencies that agree well with the frequencies obtained using ELFINI reported in Ref. 5.

### Sensitivity Derivatives of the Flutter Speed

The finite element modeling of the wing is performed using MSC/NASTRAN. The airfoil shape is generated by transforming a circle into an airfoil, so that shapes of varying thickness and camber can be obtained by varying the parameters. Finite element discretization of the wing skins, spars, and ribs is done, and a free vibration analysis of the wing is performed. The natural frequencies and mode shapes obtained are used to generate the generalized aerodynamic forces required for flutter analysis using FAST. The sensitivity of flutter speed to shape and modal parameters is computed using a central difference scheme in conjunction with ADIFOR.

#### Airfoil Coordinates for the Wing

It is beneficial if the airfoil shape generation for the wing cross section is parameterized so that shapes of varying thickness and camber can be generated. To generate the coordinates of the wing cross section, a transformation of a circle into an airfoil is carried out using the Joukowski transformation. The equation of the circle in the  $\zeta$ -plane shown in Fig. 4 is

$$(\xi - p)^2 + (\eta - q)^2 = a^2 \quad (1)$$

with center at  $\mu = p + iq$  and radius  $a$ .

For points on the circle,

$$\left. \begin{aligned} \xi &= p + a \cos \theta \\ \eta &= q + a \sin \theta \end{aligned} \right\} \quad 0 \leq \theta \leq 2\pi \quad (2)$$

Therefore,

$$\zeta = \xi + i\eta = (p + a \cos \theta) + i(q + a \sin \theta) \quad (3)$$

The circle is transformed into an airfoil in the  $z$  plane using the Joukowski transformation

$$z = \zeta + (c^2/\zeta) \quad (4)$$

Substituting for  $\zeta$  from Eq. (3) and denoting

$$D = p^2 + q^2 + a^2 + 2a p \cos \theta + 2a q \sin \theta \quad (5)$$

we have

$$\frac{z}{c} = \left( \frac{p}{c} + \frac{a}{c} \cos \theta \right) \left( 1 + \frac{c^2}{D} \right) + i \left( \frac{q}{c} + \frac{a}{c} \sin \theta \right) \left( 1 - \frac{c^2}{D} \right) \quad (6)$$

A number of different airfoil shapes can be generated by varying the values of  $p$  and  $q$ . Choosing  $p = -c/12$  and  $q = 0$ , the airfoil generated is shown in Fig. 4.

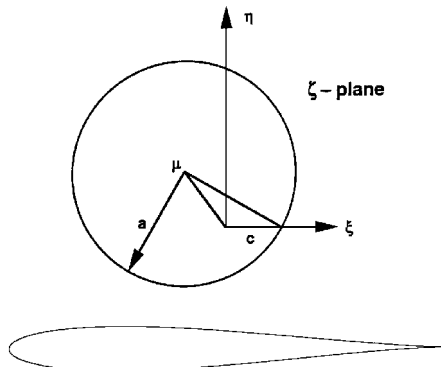


Fig. 4 Airfoil generated by transformation of a circle.

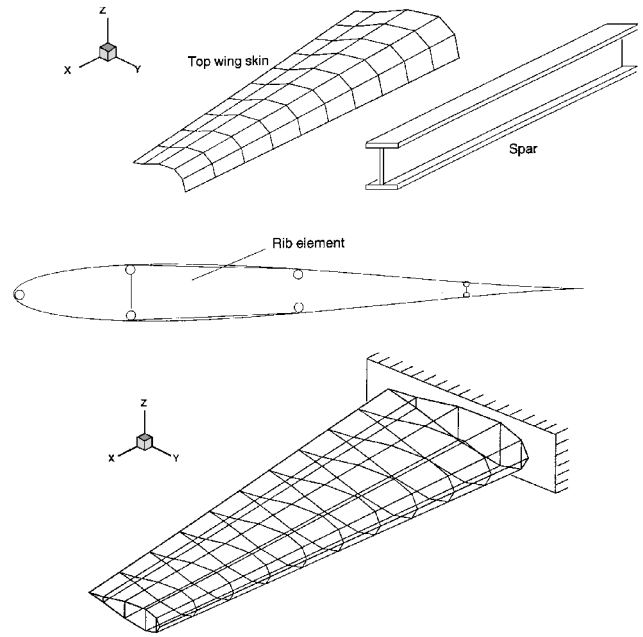


Fig. 5 Finite element discretization of the wing.

#### Free Vibration Modes of the Wing

Before performing a flutter analysis using the lifting-surface unsteady aerodynamic program FAST, the free vibration analysis of the wing structure has to be performed. The finite element discretization of the wing is shown in Fig. 5, with the coordinates of the upper and lower skins of the wing obtained from Eq. (6). The airfoil thickness at any chord location varies linearly from the root of the wing to the tip. The wing is modeled using 4 spars (placed at  $0.05c$ ,  $0.2c$ ,  $0.5c$ , and  $0.8c$  location) and 10 ribs (placed equidistant along the span). A total of 190 CQUAD4 and CTRIA3 shell elements and 200 CBAR beam elements were used to model the wing structure. The dimensions of the wing are as follows: wing span  $L = 5$  m, area  $A = 7.5$  m<sup>2</sup>, root chord  $C_r = 2$  m, tip chord  $C_t = 1$  m, wing skin thickness  $t = 3$  mm, area of beam elements  $A_b = 75$  mm<sup>2</sup>, Young's modulus  $E = 70$  GPa, Poisson's ratio  $\nu = 0.3$ , and material density  $\rho = 2700$  kg/m<sup>3</sup>.

The natural frequencies and the mode shapes of the wing are obtained from NASTRAN and the first six frequencies and the corresponding free vibration modes of the wing are given in Fig. 6.

#### Flutter Calculations Using FAST

Flutter calculations are performed using FAST,<sup>7</sup> a system of programs based on the subsonic kernel function lifting-surface aerodynamic theory. The free vibration modes of the wing are fed into FAST, which solves the subsonic downwash integral equation and computes the generalized aerodynamic forces on the wing. The flutter speed of the wing is obtained using a  $V$ - $g$  type of solution. The generalized aerodynamic forces are determined for a specific Mach number and for a range of values of the reduced frequency for the specified downwash distribution. These values are then interpolated to get aerodynamic forces for closely spaced values of the reduced frequency. The flutter equation solved by the program is

$$[\omega^2 - \omega_i^2(1 + ig)]M_i q_i + \sum_{j=1}^n A_{ij} q_j = 0, \quad i = 1, n \quad (7)$$

where  $\omega$  is the vibration frequency,  $\omega_i$  is the frequency of the  $i$ th natural vibration mode,  $M_i$  is the generalized mass associated with the  $i$ th natural vibration mode,  $g$  is the incremental damping,  $A_{ij}$  are the generalized aerodynamic forces resulting from the pressure induced by the  $j$ th mode acting through the displacements of the  $i$ th mode, and  $q_i$  is the  $i$ th component of the flutter eigenvector.

In terms of the nondimensional generalized aerodynamic forces  $A_{ij}$ , the preceding equation can be written as an eigenvalue problem in the form

$$\sum_{j=1}^n (C_{ij} - \delta_{ij} \Omega) q_j = 0, \quad i = 1, n \quad (8)$$

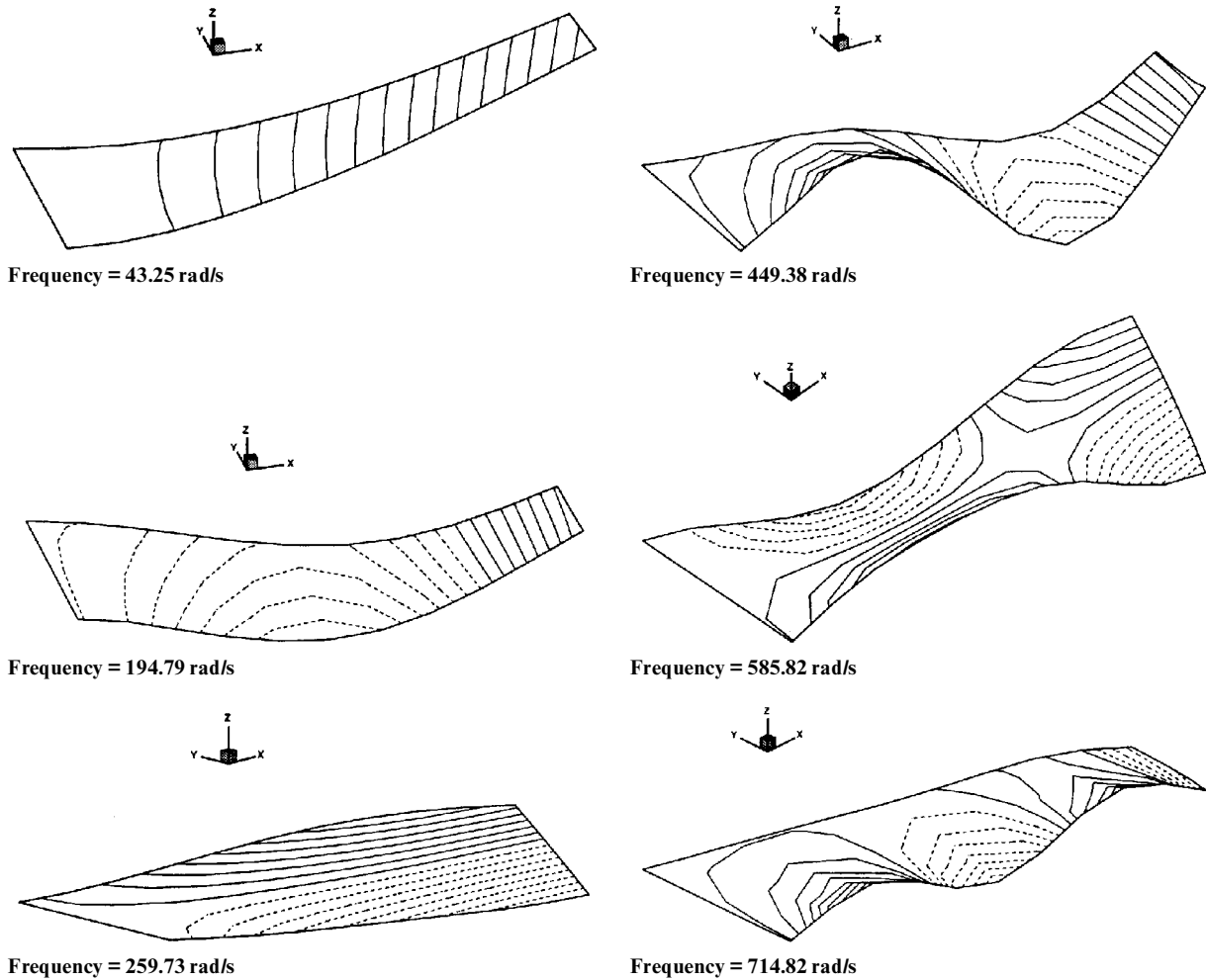


Fig. 6 Mode shapes of the wing.

where the eigenvalue  $\Omega$  is given by

$$\Omega = (\omega_0 b_0 / V)^2 (1 + i g) \quad (9)$$

and

$$C_{ij} = \left( \frac{\omega_0}{\omega} \right)^2 \left[ \frac{\rho b_0^3 \bar{A}_{ij}}{2 M_i} + \delta_{ij} k^2 \right] \quad (10)$$

where  $\omega_0$  is a reference frequency;  $b_0$  is the reference length, usually root semichord;  $k$  is the reduced frequency;  $\rho$  is the air density; and  $V$  is the airspeed.

The preceding eigenvalue problem is solved for a range of values of the reduced frequency and monitored for crossings on the  $V$ - $g$  plane when the incremental damping  $g$  goes to zero. At each of these crossings, the values of the airspeed and the frequency are noted. The critical flutter speed is the lowest speed at which the damping of the structure goes to zero.

### Results and Discussion

To perform the aeroelastic analysis using FAST, six vibration modes of the wing are used. The modal information from MSC/NASTRAN finite element analysis is input into FAST to generate the flutter speed. The flutter speed for the wing is found to be 425.296 m/s. The sensitivity analysis is carried out in two steps: a finite difference calculation followed by automatic differentiation (ADIFOR). One of the shape parameters of the wing is perturbed by a small positive value, and the free vibration modes of the new wing configuration are obtained from MSC/NASTRAN. Again, the shape parameter is perturbed by a small negative value from its nominal value, and modal analysis is carried out. Note here that the repeated finite element calculation is not very expensive because the analysis

can be performed to yield only a certain number of modes, which are required for the flutter analysis, rather than compute all of the frequencies. The derivatives of the modal frequency and mode shapes are calculated using a central difference scheme

$$\frac{\partial f}{\partial x} = \frac{f(x + \Delta x) - f(x - \Delta x)}{2\Delta x} \quad (11)$$

When the modal information is read into FAST for flutter analysis, the corresponding derivative information is also read in. These derivative values are then propagated, and the derivatives of the subsequent active variables are calculated using ADIFOR.

The sensitivity of flutter speed to shape parameters, namely, aspect ratio, area, taper ratio, and sweep angle is plotted in Figs. 7–10 along with the flutter speed calculated from a reanalysis by changing one shape parameter at a time for the wing at  $M = 0.6$ . When one parameter is changed, all of the other parameters are held constant. This amounts to generating a new set of grid points for the wing corresponding to an independent change in one of the parameters. The shape sensitivity derivatives give the trend that can be expected in the flutter speed variation for small changes in shape parameters about the baseline configuration. By performing one sensitivity calculation at the baseline, this method gives a linear approximation to the flutter speeds of the wing for changes in the wing shape parameters about the baseline. This information is useful for preliminary design purposes, as it avoids the necessity of a reanalysis for small changes in any of the shape parameters. The weight changes that accompany these changes in the design parameters will be particularly interesting in an optimization study. Is there any weight penalty that one would have to pay to get an aeroelastically efficient design? In such cases, one might be interested in looking at the sensitivity of the wing weight to changes in the shape and sizing parameters.

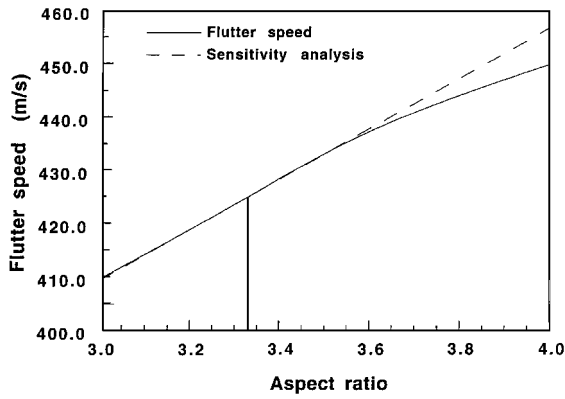


Fig. 7 Flutter speed vs aspect ratio:  $M = 0.6$ ,  $AR = 3.33$ , area =  $7.5 \text{ m}^2$ ,  $TR = 0.5$ , and sweep =  $15 \text{ deg}$ .

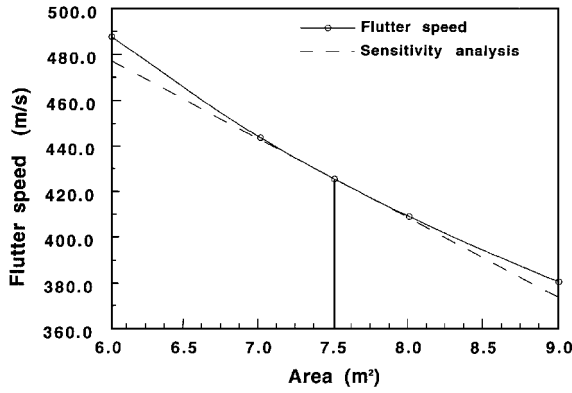


Fig. 8 Flutter speed vs area:  $M=0.6$ ,  $AR=3.33$ , area =  $7.5 \text{ m}^2$ ,  $TR = 0.5$ , and sweep =  $15 \text{ deg}$ .

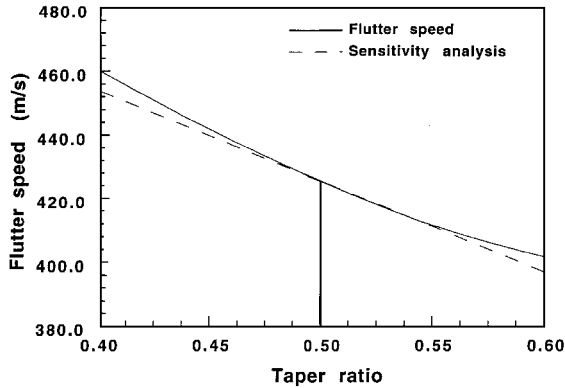


Fig. 9 Flutter speed vs taper ratio:  $M = 0.6$ ,  $AR = 3.33$ , area =  $7.5 \text{ m}^2$ ,  $TR = 0.5$ , and sweep =  $15 \text{ deg}$ .

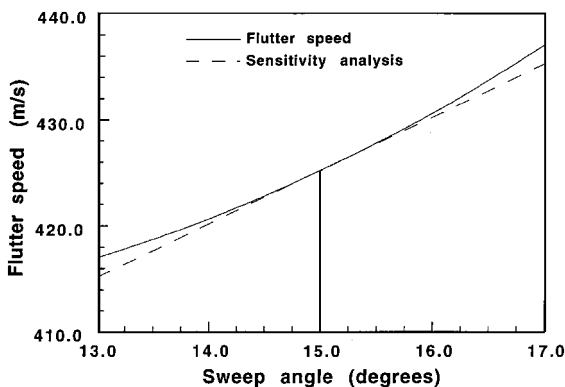


Fig. 10 Flutter speed vs sweep angle:  $M = 0.6$ ,  $AR = 3.33$ , area =  $7.5 \text{ m}^2$ ,  $TR = 0.5$ , and sweep =  $15 \text{ deg}$ .

Complex wing structures are often modeled with a large number of degrees of freedom, and a vibration analysis yields a large number of free vibration modes. A certain number of these modes have to be provided to FAST to generate the generalized aerodynamic forces required for flutter analysis. Some of these modes do not actively participate in the flutter, and using several modes to determine flutter instability leads to a higher computational cost. In situations, where the natural frequencies and mode shapes of the wing are measured from experiments, one has large amount of modal data and has to determine the number of modes that are required for reasonably estimating the flutter speed. One could make a judicious choice of the number of modes that are required for flutter analysis, based on the sensitivity derivatives of the flutter speed with respect to the modal parameters of the wing.

The sensitivity of flutter speed to modal parameters are obtained using ADIFOR. The derivatives of the flutter speed with respect to natural frequencies of the wing are shown in Fig. 11. Six modes were used for the flutter analysis. It can be seen that if the third natural frequency is increased by  $1 \text{ rad/s}$ , then the flutter speed increases by  $2.16 \text{ m/s}$ . It is also seen that higher modes do not contribute much to the flutter. The derivatives of the flutter speed with respect to generalized mass are given in Fig. 12 and the flutter speed sensitivity to the real and imaginary parts of the generalized aerodynamic forces (GAF) is given in Fig. 13. The  $(i, j)$  term in Fig. 13 stands for the nondimensional generalized aerodynamic force resulting from the pressure induced by the  $j$ th mode acting through the displacements of the  $i$ th mode. The sensitivities of flutter speed with respect to modal parameters give an estimate of the importance of a particular mode to flutter.

To obtain a quantitative estimate of the contribution of a particular mode to flutter, one can use the sensitivity information, which gives the variation of flutter speed with the natural frequency, generalized mass, and real and imaginary parts of the generalized aerodynamic forces associated with that mode. It is possible to construct a logarithmic derivative and sum up the absolute values of these derivatives, which reflects the change in flutter speed due to changes in modal parameters associated with a particular mode. Having obtained all of the derivatives one could construct a parameter  $P_i$  for each mode  $i$  given by

$$P_i = \left| \frac{\omega}{V_f} \frac{\partial V_f}{\partial \omega} \right| + \left| \frac{M_i}{V_f} \frac{\partial V_f}{\partial M_i} \right| + \sum_{j=1}^N \left[ \left| \frac{\text{Re}(Q_{ij})}{V_f} \frac{\partial V_f}{\partial \text{Re}(Q_{ij})} \right| + \left| \frac{\text{Im}(Q_{ij})}{V_f} \frac{\partial V_f}{\partial \text{Im}(Q_{ij})} \right| \right] \quad (12)$$

where  $V_f$  is the flutter speed,  $\omega$  is the natural frequency,  $M_i$  is the generalized mass, and  $\text{Re}(Q_{ij})$  and  $\text{Im}(Q_{ij})$  are the real and imaginary parts, respectively, of the generalized aerodynamic forces for an aeroelastic analysis using  $N$  vibration modes. The values of this parameter  $P_i$  for the nine modes used in the analysis are given in Table 2. The decreasing values of this parameter for higher modes indicate that the flutter speed is not sensitive to higher modes, and the inclusion of these modes is not very significant for a flutter calculation.

The attraction of ADIFOR is its capability of generating derivative information with respect to a multitude of parameters in one run and precludes the need for making individual runs for different parameters at a higher computational cost. The greater is the number of input parameters the greater the savings using ADIFOR. A conventional forward or backward difference scheme will require one evaluation of the output variable at the baseline configuration and

Table 2 Sum of the absolute values of the logarithmic derivatives

Mode $i$	Parameter $P_i$
1	0.7359696E_01
2	0.3695617E+00
3	0.1656248E+01
4	0.1375119E_02
5	0.1139148E_01
6	0.9932521E_03

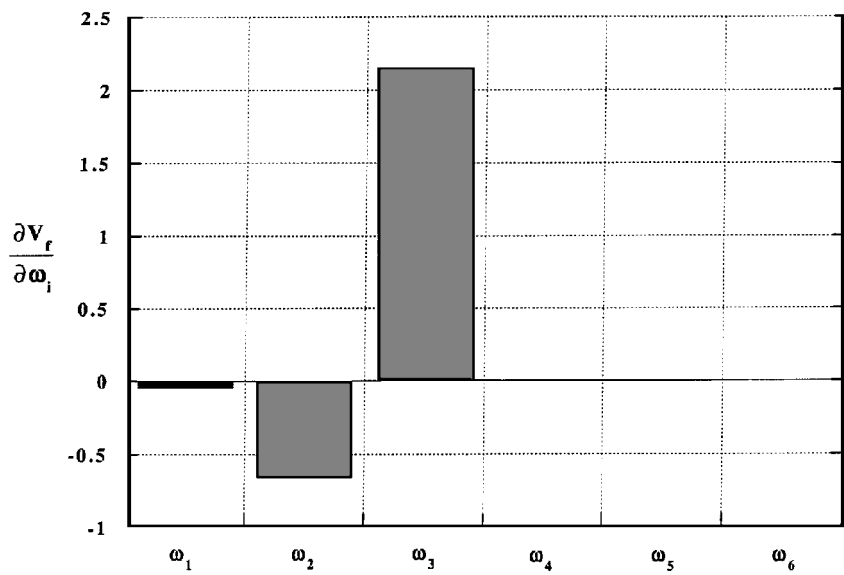


Fig. 11 Flutter speed sensitivity to natural frequency in meters per second per radians per second:  $M = 0.6$ ,  $AR = 3.33$ , area =  $7.5 \text{ m}^2$ ,  $TR = 0.5$ , and sweep = 15 deg.

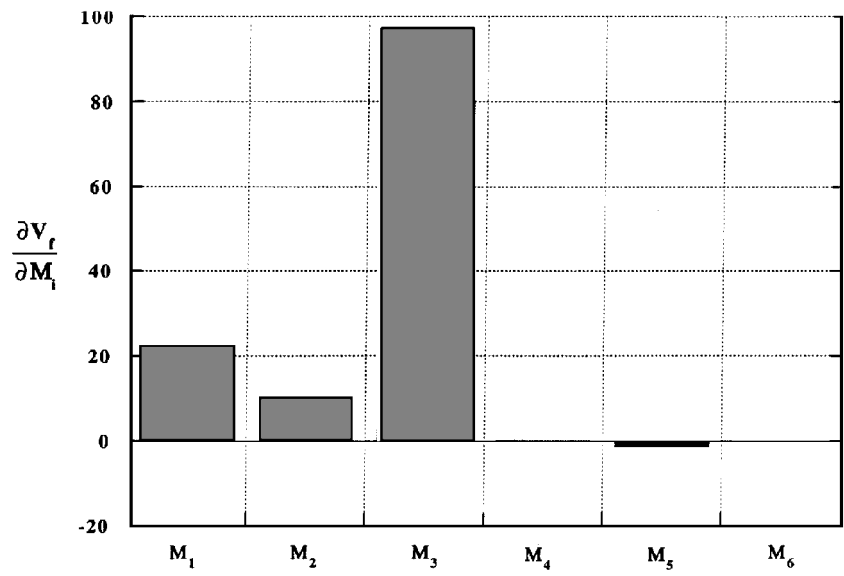


Fig. 12 Flutter speed sensitivity to generalized mass in meters per second per kilogram:  $M = 0.6$ ,  $AR = 3.33$ , area =  $7.5 \text{ m}^2$ ,  $TR = 0.5$ , sweep = 15 deg.

evaluations at perturbed values of each independent variable. Thus, for four independent variables such as aspect ratio, area, taper ratio, and sweep angle, this amounts to five independent runs. Similarly, a central difference scheme would require nine independent runs. When using ADIFOR, the derivative information at each stage of the computation is propagated as the analysis progresses, and when the analysis is complete, the sensitivity results are readily available.

The automatic differentiation software ADIFOR generates an augmented code with the analysis source code provided. However, one may have to modify these files sometimes. If intermediate outputs are written onto a file in the program, the corresponding derivative values will also have to be written onto an output file, so that these can be read in wherever required so that the derivative values are propagated throughout the program. Some interesting observations were made about the augmented Fortran code. Sometimes, there are lines in the original code where you set a very small number to zero (which essentially means you have set that variable to a constant value of zero). When ADIFOR encounters that Fortran statement, it sets the derivative of that variable to zero (because the derivative of a constant is zero). But actually, even though that variable is a small number, its derivative is not necessarily small, and the erroneous derivative information will be propagated throughout the rest of the code, giving meaningless numbers. Another interesting observation

was the use of equivalence statements and how the derivative information is stored in two equivalent arrays. When a new set of numbers is read into the array, care should be taken to see that its derivative is set to zero. Otherwise, the old information in the derivatives array will be used.

The sensitivity information is useful in the design stage and reduces the cost of the design process. These could be incorporated into the design process to generate an optimum design. Because source codes cannot be accessed for the commercial finite element software like MSC/NASTRAN, finite differencing schemes must be used to get sensitivities. However, once the nominal parameters are chosen for the wing, the results can be generated at the baseline configuration. When one of the parameters is perturbed for a finite difference calculation, new coordinates for the wing are generated and, hence, a new set of grid points, will replace the old set of grid points, and this can be easily achieved by retaining the same number of nodes and the same number of elements as before. Once the structural dynamic analysis is complete and the finite difference derivatives are available, these are input into the augmented flutter code, and the derivatives are propagated to obtain the final sensitivity results. Based on the optimization algorithm and the constraints of the optimization, a new set of design variables will be produced and the cycle is repeated until convergence.

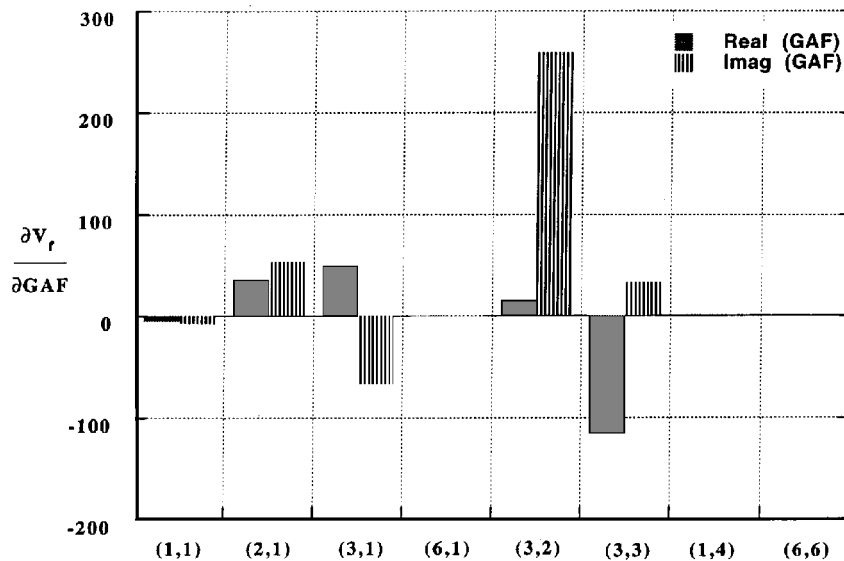


Fig. 13 Flutter speed sensitivity to nondimensional GAF in meters per second:  $M = 0.6$ ,  $AR = 3.33$ , area =  $7.5 \text{ m}^2$ ,  $TR = 0.5$ , and sweep =  $15 \text{ deg}$ .

### Concluding Remarks

Flutter calculations for a wing are performed using a finite element structural model using MSC/NASTRAN, a lifting-surface unsteady aerodynamic theory, and a  $V$ - $g$  type of solution using FAST. The sensitivity of flutter speed to shape and modal parameters have been obtained using a combination of central difference scheme and ADIFOR. The shape sensitivity derivatives give a linear approximation to the flutter speed curve over a range of values of the shape parameter about the baseline configuration. The shape derivatives of the flutter response of a wing would be very useful to a designer in the initial design phase, thus avoiding the necessity of a reanalysis for small changes in the design parameters. The sensitivity derivatives of the flutter response to modal parameters are useful for identifying the modes that are important aeroelastically. The logarithmic derivatives constructed from the sensitivity information of the flutter speed derivatives with respect to modal parameters give a quantitative estimate of the number of modes that are required for reasonably evaluating the flutter speed.

### Acknowledgments

The work presented here is a part of the work done in the project sponsored by NASA Langley Research Center under Grant NAG-1-1411 to Virginia Polytechnic Institute and State University. The authors would like to thank Jean-Francois M. Barthelemy, Robert M. Bennett, and E. Carson Yates of NASA Langley Research Center

for their ideas and valuable suggestions. The suggestions by the reviewers for revising this manuscript are gratefully acknowledged.

### References

- <sup>1</sup>Bischof, C., "Principles of Automatic Differentiation," ADIFOR Workshop, NASA Langley Research Center, Hampton, VA, Sept. 1993.
- <sup>2</sup>Kapania, R. K., Bergen, F. D., and Barthelemy, J.-F. M., "Shape Sensitivity Analysis of Flutter Response of a Laminated Wing," *AIAA Journal*, Vol. 29, No. 4, 1991, pp. 611, 612.
- <sup>3</sup>Kapania, R. K., and Issac, J. C., "Sensitivity Analysis of Aeroelastic Response of a Wing in Transonic Flow," *AIAA Journal*, Vol. 32, No. 2, 1994, pp. 350–356.
- <sup>4</sup>Issac, J. C., Kapania, R. K., and Barthelemy, J.-F. M., "Sensitivity Analysis of Flutter Response of a Wing to Shape and Modal Parameters," *AIAA Journal*, Vol. 33, No. 10, 1995, pp. 1983–1986.
- <sup>5</sup>Livne, E., "Equivalent Plate Structural Modeling for Wing Shape Optimization Including Transverse Shear," *AIAA Journal*, Vol. 32, No. 6, 1994, pp. 1278–1288.
- <sup>6</sup>Anon., "MSC/NASTRAN Version 67," User's Manual, MacNeal-Schwendler Corp., 1991.
- <sup>7</sup>Desmarais, R. N., and Bennett, R. M., "User's Guide for a Modular Flutter Analysis Software System," NASA TM 78720, May 1978.
- <sup>8</sup>Turner, M. J., Martin, H. C., and Weikel, R. C., "Further Development and Applications of the Stiffness Method," *Matrix Methods of Structural Analysis*, AGARDograph 72, edited by F. B. de Veubeker, Pergamon, Oxford, England, UK, 1964, pp. 203–266.

A. Berman  
Associate Editor